Complex Dynamics of Blackouts in Power Transmission Systems

B. A. Carreras and V. E. Lynch
Oak Ridge National Laboratory, Oak Ridge, TN 37831
I. Dobson
ECE Dept., University of Wisconsin, Madison, WI 53706 USA
D. E. Newman
Physics Dept., University of Alaska, Fairbanks, AK 99775 USA

Abstract

A model has been developed to study the complex global dynamics of a series of blackouts in power transmission systems. This model includes a simple level of self-organization by incorporating the growth of power demand, the engineering response to system failures, and the upgrade of generator capacity. Two types of blackouts have been identified, each having different dynamical properties. One type of blackout involves the loss of load due to transmission lines reaching their load limits but no line outages. The second type of blackout is associated with multiple line outages. The dominance of one type of blackout over the other depends on operational conditions and the proximity of the system to one of its two critical points. The model shows a probability distribution of blackout sizes with power tails similar to that observed in real blackout data from North America.

I. Introduction

Power transmission systems are complex systems that evolve over years in response to the economic growth of the country and to continuously increasing power demand. The evolution and reliability of these systems are leading engineering accomplishments of the last century that underpin developed societies. Nevertheless, widespread disturbances of power transmission systems that have significant cost to society are consistently present. An analysis of blackouts[1] done in the 1970s indicated that the average frequency of blackouts in the United States was one every 14 days. More recent analyses[2,3] of 15 years of North American Electrical Reliability Council (NERC) data on blackouts of the North American power grid[4] gave an average frequency of blackouts of one every 13 days. Furthermore, these analyses show that the distribution of blackout sizes has a power tail with an exponent of about -1.3 ± 0.2. These results indicate that the probability of large blackouts is relatively high. Indeed, although large blackouts are rarer than small blackouts, it can be argued that their higher societal costs, together with their relatively high probability, makes the risk of large blackouts comparable to or exceeding the risk of small blackouts.[5]

Individual blackouts are triggered by random events ranging from equipment failures and bad weather to vandalism.[4] The blackouts typically become widespread by a series of cascading events. However, we emphasize that individual blackouts occur in a power transmission system that is slowly and dynamically evolving in its design, configuration and operation. For example, the loading of system components relative to their maximum loading is a key factor governing the propagation of component failures and this loading evolves as the system components or operational policies are upgraded. The existence of a power tail in the distribution of blackouts suggests that the underlying cause of large-scale blackouts may lie in the existence of correlations induced by the proximity to the critical point. The size of the blackout is are unrelated to the particular triggering event that initiated blackout.

To investigate such a possibility, we propose a model for power transmission systems[6,7] that involves not only the dynamics of the generator dispatch but also the evolution of the system under a continuous increase in demand. This model shows how the slow opposing forces of load growth and network upgrades in response to blackouts

could self-organize the power system to a dynamic equilibrium. Blackouts are modeled by overloads and outages of transmission lines determined in the context of linear programming (LP) dispatch of a DC load flow model. This model shows complex dynamical behaviors and has a variety of transition points as a function of increasing power demand.[8] Some of these transition points have the characteristic properties of a critical transition. That is, when the power demand is close to a critical value, the probability distribution function (PDF) of the blackout size has an algebraic tail, and the system changes sharply across the critical point. The risk of a global blackout increases sharply at the critical transition.

The fact that, on one hand, there are critical points with maximum power flow through the network and, on the other hand, there is a self-organization process that tries to maximize efficiency and minimize risk, may lead to a power transmission model governed by self-organized criticality (SOC).[9] Such a possibility was first explored with a simple cellular automaton model[10] that incorporates neither the circuit equations nor the type of long-term dynamics discussed above. In this paper, we study the dynamical properties of a power transmission model[6,7] that incorporates these two components.

There have been some other complex system approaches to power system blackouts. In the most closely related work, Chen and Thorp[11,12] modeled power system blackouts using DC load flow and LP dispatch and represent in detail hidden failures of the protection system. The distribution of power system blackout size was obtained by rare-event sampling, and blackout risk assessment and mitigation methods are studied. Stubna and Fowler[13] applied a modified "Highly Optimized Tolerance" (HOT) model to fit North American blackout data for blackout sizes measured by both power shed and customers disconnected. Roy, Asavathiratham, Lesieutre, and Verghese constructed randomly generated tree networks that abstractly represent influences between idealized components.[14] Components can be failed or operational according to a Markov model that represents both internal component failure and repair processes and influences between components that cause failure propagation. The effects of the network degree of connectivity and intercomponent influences on the failure size and duration were studied. Pepyne et al.[15] also used a Markov model for discrete-state power system nodal

components but propagate failures along the transmission lines of a power systems network with a fixed probability.

Numerical simulations study the effect of the propagation probability and maintenance policies that reduce the probability of hidden failures. DeMarco[16] and Parrilo et al.[17] addressed the challenging problem of determining cascading failure due to dynamic transients by using hybrid nonlinear differential equation models. Demarco used Lyapunov methods applied to a smoothed model; Parrilo et al. used Karhunen-Loeve and Galerkin model reduction.

The operation of power transmission systems results from a complex dynamical process in which a diversity of opposing forces regulate both the maximum capabilities of the system components and the loadings at which they operate. These forces enter in a highly nonlinear manner and may cause a self-organization process to be ultimately responsible for the regulation of the system. This view of a power transmission system considers not only the engineering and physical aspects of the power system, but also the engineering, economic, regulatory, and political responses to blackouts and increases in load power demand. A detailed incorporation of all these aspects of the dynamics into a single model would be extremely complicated if not intractable due to the human interactions involved. However, it is useful to consider simplified models with some approximate overall representation of the opposing forces in order to gain some understanding of the complex dynamics in such a self-organized framework and the consequences for power system planning and operation.

The rest of this paper is organized as follows. In Sect. 2, we introduce a dynamical model of power transmission system evolution over long time scales. Details of the power flow model and of the fast time scale dynamics are provided in Appendix A. In Sect. 3, numerical results of the model are reported with an analysis of the time and space correlations introduced by the dynamics. In Sect. 4, we analyze the effect of changing the ratio of generator capacity margin to maximum load fluctuation. This ratio allows the separation of the dynamics into two different regimes. The conclusions of this paper are given in Sect. 5.

2. Dynamical model for power transmission

In modeling the dynamics of power transmission systems, we consider two intrinsic time scales. There is a slow time scale, of the order of days to years, over which load power demand slowly increases. Over this time scale, the network is upgraded in engineering responses to blackouts and in providing more generator power in response to demand. As we shall see, these slow opposing forces of load increase and network upgrade self-organize the system to a dynamic equilibrium. The dynamical properties of this model are the main topic of this paper. In power transmission systems, there is also a fast time scale, of the order of minutes to hours, over which power is dispatched through the network within which (depending on the conditions of the network) cascading overloads or outages may lead to a blackout.

Over the fast time scale, we solve the standard DC power flow equation for a given distribution of load demand. We use the standard LP method[18–20] with the usual constraints on generating power capability and transmission line limits to solve the generator power dispatch. An example of a power transmission network used in these studies is the IEEE 118 bus network[21] shown in Fig. 1. Details on the fast dynamics can be found in Refs. 6 and 7 and a summary description is given in Appendix A.

In any network, the network nodes (buses) are either loads (L) (gray squares in Fig. 1), or generators (G), (black squares in Fig. 1). The power P_{i} injected at each node is positive for generators and negative for loads, and the maximum power injected is $P_i^{\max}$. The transmission line connecting nodes i and j has power flow F_{ij}, maximum power flow $F_{ij}^{\max}$, and impedance z_{ij}. There are N_{l} lines and $N_N = N_G + N_L$ total nodes, where N_{G} is the number of generators and N_{L} is the number of loads.

The slow dynamics proposed in Refs. 6 and 7 has three components: (1) the growth of the demand, (2) response to blackouts by upgrades in the grid transmission capability and (3) response to increased demand by increasing maximum generator power. These components of the model are translated into a set of simple rules. We simplify the time scale by regarding one blackout to be possible each day at the peak loading of that day. At the beginning of the day t, we apply the following rules

1. The demand for power grows. All loads are multiplied by a fixed parameter λ that represents the daily rate of increase in electricity demand. On the basis of past electricity consumption in the United States, we estimate that λ = 1.00005. This value corresponds to a yearly rate of 1.8%.

$$P_i(t) = \lambda P_i(t-1) \quad \text{for } i \in L \quad . \tag{1}$$

To represent the daily local fluctuations in power demand, all power loads are multiplied by a random number *r*, such that $2-\gamma \le r \le \gamma$, with $0 \le \gamma \le 2$.

2. The power transmission grid is improved. We assume a gradual improvement in the transmission capacity of the grid in response to outages and blackouts. This improvement is implemented through an increase of $F_{ij}^{\max}$ for the lines that have overloaded during a blackout. That is,

$$F_{ij}^{\max}(t) = \mu F_{ij}^{\max}(t-1), \tag{2}$$

if the line *ij* overloads during a blackout. We take μ to be a constant.

It is customary for utility engineers to make prodigious efforts to avoid blackouts, and especially to avoid repeated blackouts with similar causes. These responses to blackouts occur on a range of time scales longer than one day. Responses include repair of damaged equipment, more frequent maintenance, changes in operating policy away from the specific conditions causing the blackout, installing new equipment to increase system capacity, and adjusting or adding system alarms or controls. The responses reduce the probability of events in components related to the blackout, either by lowering their probabilities directly or by reducing component loading by increasing component capacity or by transferring some of the loading to other components. The responses are directed toward the components involved in causing the blackout. Thus the probability of a similar blackout occurring is reduced; at least until load growth degrades the improvements that were made. There are

similar but less intense responses to unrealized threats to system security, such as near misses and simulated blackouts.

Here, we have simplified all engineering responses into a single parameter μ. This is a crude representation of all these responses to a blackout. The response is modeled as happening on the next day, but the effect is eventually cancelled by the slow load increase. Because of the disparity between these two time scales, it does not seem crucial to have an accurate estimate of the response time, and the one-day time scale may be reasonable.

3. The maximum generator power is increased as a response to the load demand as follows
   (a) The increase in power is quantized. This may reflect the upgrade of a power plant or added generators. The increase is taken to be a fixed ratio to the total power. Therefore, we introduce the quantity

$$\Delta P_a \equiv \kappa\left(P_T / N_G\right) \ , \tag{3}$$

   where, P_T is the total power demand and κ is a parameter that we have taken to be a few percent.

   (b) To be able to increase the maximum power in node *j*, the sum of the power flow limits of the lines connected to *j* should be larger than the existing generating power plus the addition at node *j*. This requirement maintains the coordination of the maximum generator power ratings with the line ratings.

   (c) A second condition to be verified before any maximum generator power increase is that the mean generator power margin has reached a threshold value. That is, we define the mean generator power margin at a time *t* as

$$\frac{\Delta P}{P} = \frac{\sum_{j \in G} P_j - P_0 e^{(\lambda - 1)t}}{P_0 e^{(\lambda - 1)t}} \ , \tag{4}$$

where P_0 is the initial power load demand.

(d) Once condition (c) is verified, we choose a node at random to test condition (b). If the chosen node verifies condition (b), we increase its power by the amount given by Eq. (3). If condition (b) is not verified, we choose another node at random and iterate. After power has been added to a node, we use Eq. (4) to recalculate the mean generator power margin and continue the process until $\Delta P/P$ is above the prescribed quantity $\left(\Delta P/P\right)_c$.

4. We also assign a probability p_0 for a random outage of a line. This value represents possible failures caused by phenomena such as accidents and weather related events.

After applying these four rules to the network, we look for a solution of the power flow problem by using LP, as described in Appendix A.

It is also possible to introduce a time delay between the detection of a limit in the generation margin and the increase in maximum generator power. This delay would represent construction time. However, the result is the same as increasing the value of κ in Eq. (3), which can also give an alternative interpretation for κ.

Five basic parameters control the dynamics of this model. One is the rate of increase in power demand, λ, which we keep fixed at 1.8% per year on the basis of the averaged value for the U.S. grid in the last two decades.[22] A second parameter is the improvement rate of the transmission grid, μ. This is not an easy parameter to estimate. However, once μ is given, there is a self-regulation process by which the system produces the number of blackouts that would stimulate the engineering response needed to meet demand. This is a necessary condition for the dynamical equilibrium of the system. The rate of increase in power demand for the overall system is essentially given by $R_D \approx (\lambda - 1)N_L$. The system response is $R_R \approx (\mu - 1) f_{blackout} \langle \ell_o \rangle N_L$, where $f_{blackout}$ is the frequency of blackouts and $\langle \ell_o \rangle$ is a weighted average of the number of lines overloaded during a blackout. Dynamical equilibrium implies that $R_D = R_R$. That is, the increase in demand and the corresponding increase in power supply must be matched by improvements in the transmission grid. Because those improvement are in response to real or simulated

blackouts, this relation implies that μ must be greater than λ; otherwise, the system would be collapsing with constant blackouts. In the numerical calculations and for the value of the growth demand of 1.8% per year, we found that, in order to avoid this collapse regime, μ must be > 1.01. In the present calculations, we keep this parameter in the range 1.01 to 1.1. In this regime, results depend weakly on this parameter.

A third parameter is the ratio Γ of the minimal generator power margin $\left(\Delta P/P\right)_c$ to the maximum fluctuation of the load demand $g \equiv \mathrm{Max}\left(\left[\left(P_D - P_0 e^{(\lambda-1)t}\right)/\left(P_0 e^{(\lambda-1)t}\right)\right]^2\right)^{1/2}$.

$$\Gamma = \left(\Delta P/P\right)_c / g \ , \tag{5}$$

where, P_D is the actual load demand that fluctuates around the mean value and g is simply related to the parameter γ. The parameter Γ is the main parameter varied in the calculations presented here. The generator power capability margin has a wide variation over the years, but an estimated mean value[22] falls into the range of 15% to 30%.

The fourth parameter is the probability of an outage caused by a random event (p_0). This parameter can be used to partially control the frequency of blackouts, although there is not a linear relation between them. The fifth parameter is the probability for an overloaded line to undergo an outage (p_1). We keep this parameter in the range $0.1 \le p_1 \le 1.0$.

Each calculation is done for a specific network configuration. We will use idealized tree networks, which were discussed in Ref. 8, as well as more realistic networks, such as the IEEE 118 bus network depicted in Fig. 1.

The time evolution of a power transmission system by this model leads to a steady-state regime. Here "steady state" is defined with relation to the slow dynamics of the blackouts because the power demand is constantly increasing, as shown in Fig. 2. The time evolution in the model shows a transient period followed by steady-state evolution. This is illustrated in Fig. 2, where we have plotted the number of blackouts per 300 days as a function of time. We can see a slight increase in the average number of blackouts during the first 20,000 days. This transient period is followed by a steady state where the

number of blackouts in an averaged sense is constant. The properties in the slow transient are not very different from those in the steady state. However, for statistical analysis, it is better to use the steady-state information. The length of the transient depends on the rate of growth in power demand. In the following calculations, we evaluate the blackout statistics by ignoring the initial transients and doing the calculations for a time period of 80,000 days in a steady state. Of course, the use of steady-state results is driven by the need for large statistical samples. It is arguable whether the real electric power grid ever reaches a steady state.

3. Dynamical evolution of the power transmission model

Looking at the time evolution of the different parameters that characterize the blackouts, one observes a noisy signal that could be taken as random. One could think that this is the situation because many of the blackouts are triggered by random events with probability p_0. However, that is not the case. There are significant space and time correlations resulting from the dynamics of the power transmission model.

Let us first consider the time correlations. A simple way of studying these correlations is by calculating the Hurst exponent[23] of time series of blackout sizes. Here, we consider two measures of the size of a blackout. One is the load shed during a blackout normalized to the total power demand; the other is the number of line outages during a blackout.

We use the R/S method[24] to calculate the Hurst exponent. An example of the results is shown in Fig. 3. For times of the order of a few days and a few years, both series show weak persistency. They have the same Hurst exponent ($H = 0.55 \pm 0.02$). This result is close to the one obtained in the analysis[2] of NERC data on blackouts of the North American power grid.[4] In this range of time scales, the value of the exponent does not depend on the value of Γ. For longer times, each time series shows a different behavior. The load shed has a nearly random character with $H = 0.5$ for $\Gamma < 1$. For $\Gamma > 1$, the value of H decreases and in many cases is below 0.5. For these longer time scales, the time series of the number of line outages has a clear antipersistent character with H ranging

from 0.2 to 0.4, depending on the network structure. In Fig. 4, the value of H resulting from a fit of R/S in the time range $600 \leq t \leq 10^5$ is given as a function of Γ for three of the tree networks and for the IEEE 118 bus network. Antipersistency in the time sequence of number of line outages can be expected from the model. Blackouts with a large number of line outages happen rarely, only once every few years. When they happen, there is a great deal of repair and enhancement of many transmission lines. As a consequence, blackouts with a large number of line outages become less probable after one of those events. Therefore, there is antipersistency at that time scale. In the present model, load shed does not have a direct impact on the repair and upgrade of the system. Therefore, time correlations are weak. As we will discuss in the next section, for $\Gamma > 1$, blackouts with large load sheds are associated with a large number of line outages. Therefore, in this Γ range we see some level of antipersistency due to the coupling of load shed and number of outage lines. The available data from NERC are limited to 15 years, and we do not have any direct way of confirming this long-term behavior of the model in the real power system.

The time lag during which the number of line outages changes from weak persistency to antipersistency is independent of the network size but depends on the repair rate (μ). As μ increases, it takes longer time lags for the change to occur. Increasing μ causes a slight increase in H, but H remains less than 0.5.

In this model, correlations are not limited to time correlations. The PDFs of the load shed and the number of line outages both have power tails. The correlations responsible for these power tails are the result of the system being near a critical point.

In Ref. 7, we studied the critical points of the power transmission model as the total load demand was varied. The slow dynamics described in Sect. 2 were not modeled. We found two types of critical points: one type was related to the limiting power flows in the transmission lines; the other type was related to the limit in the power generation. When these types of critical points are close to each other, the probability distribution of the blackout size as measured by the amount of load shed has a power tail. Away from the critical point, the PDFs do not show such power tails.

When the dynamical evolution over long time scales is included and the value of Γ is about 1, the system evolves to a situation in which these critical points are close to each other. Therefore, the PDFs of the power shed have well-developed power tails. These PDFs are shown in Fig. 5, where we have plotted the PDFs of the load shed normalized to the total power demand for three different tree configurations. These distribution functions are compared with those obtained from a load scan without dynamical evolution when the load value was at the critical point. We cannot distinguish between the two calculations; the PDFs are practically the same. In Fig. 5, we have given an arbitrary shift to the PDFs for a given size network to better observe the three different cases.

For the PDF of the power shed, the power-law-scaling region increases with the number of nodes in the network. The power decay index is practically the same for the four networks and is close to –1.2. The particular values of the decay index for each tree network are given in Table I, in which the range of the power tail region is defined as the ratio of the maximum load shed to the minimum load shed described by the power law. From the values obtained for the four networks listed in Table I, we can see that this range scales with the network size.

The PDFs plotted in Fig. 5 are totally superimposed to the PDFs of the normalized load shed obtained by the direct power demand scan in Ref. 8 near the critical points. This overlap indicates that the dynamical model described in Sect. 2 leads to operation of the system close to the critical points. A similar result has been obtained for the IEEE 118 bus network.

The forms of these PDFs, or at least their power tails, seem to have a universal character. Therefore, we can compare the PDF of the normalized load shed obtained for the largest network with the PDF of the blackouts obtained in the analysis of the 15 years of NERC data.[4] In Fig. 6, we have plotted the PDF of the NERC data together with the PDFs for the 382-node tree and IEEE 118 bus networks. We have normalized the blackout size to the largest blackout over the period of time considered. We can see that the present model, regardless of the network configuration, reproduces well the functional form obtained from the data. The level of agreement between the power tails

of these two PDFs is remarkable and indicates that the dynamical model for series of blackouts has captured some of the main features of the data.

4. Dynamical regimes

Calculations carried out with this model show the existence of two different dynamical regimes. The first regime is characterized by the low value of Γ (that is, a low generator capability margin and/or large fluctuations in the power demand). In this regime, the available power is limited and has difficulties in meeting demand. Blackouts and brownouts are frequent, but they affect few loads. In this regime, there are very few line outages. In the opposite limit, Γ is large and the blackouts are less frequent, but they tend to involve multiple line outages when they happen. This latter regime is interesting because there are many cascading events that can cause blackouts in a large part of the network. This suggests a possible separation between regimes of few failures and regimes with cascading failures.

Let us investigate in a quantitative way the separation between these two regimes by varying the parameter Γ. Varying Γ is not necessarily a realistic way of modeling the transmission system but it allows us to understand some features of the dynamics of the model. For several tree networks, we have done a sequence of calculations for different values of the minimal generator power margin $\left(\Delta P/P\right)_c$ at a constant g. We have changed this margin from 0 to 100%. For each value of this parameter, we have carried out the calculations for more than 100000 days in a steady state regime. One way of looking at the change of characteristic properties of the blackouts with Γ is by plotting the power delivered and the averaged number of line outages per blackout. For a 94-node tree network, these plots are shown in Fig. 7. We can see that at low and high values of Γ, the power served is low. In the first case, because of the limited generator power, the system cannot deliver enough power when there is a relatively large fluctuation in load demand. At high Γ, the power served is low because the number of line outages per blackout is large.

Looking at averaged quantities is not a good way of identifying the demarcation between single failures and cascading events. To have a better sense of this demarcation, we have calculated the PDF of the number of line outages per blackout. In Fig. 8, we have plotted these PDFs for different values of Γ. The calculation was done for a 94-node tree network. We can see that at very low Γ there is a clear peak at 4 outages per blackout with very low probability for blackouts with more than 10 outages per blackout. As Γ increases, a second peak at about 17 outages emerges and the high of the peak increases with Γ. At the highest Γ value, this second peak is comparable to the peak at low number outages per blackout. In Fig. 9, we have plotted the ratio of the frequency of blackouts with more than 15 outages to the mean frequency of blackouts. We can see that for $\Gamma > 1$, this ratio reaches 0.007. This gives a measure of the frequency of what we can consider large scale blackouts (more than a 16% of the whole grid). We can apply this result to the U.S. grid, taking into account that the average frequency of blackouts is one every 13 days. In the low-Γ regime, the ratio is about 0.001; this would imply that a large scale blackout is likely every 35 years. In the high-Γ regime, the ratio goes up to 0.007; this implies a frequency of one every 5 years.

5. Conclusions

The simple mechanisms introduced into the power transmission model and representing the economical and engineering responses to increasing power demands are sufficient to introduce a complex behavior in the power system. The results of the complex dynamics, time correlations, and PDFs of blackout sizes are consistent with the available data on blackouts of the North American electrical grid.

This model suggests that the real cause of the blackouts in the electric power system should not be identified just with the immediate random events that trigger them; the real cause is at a deeper level in the long term forces that drive the evolution of the power system.

An important parameter in the model, Γ, is the ratio of the generator margin capability to the maximum daily fluctuation of the loads. We do not yet have an economic model for the time evolution of Γ. This parameter allows us to classify the dynamics of the model into two regimes. At low Γ, blackouts and brownouts are frequent, and a typical blackout is characterized by very few line outages. For $\Gamma > 1$, blackouts are less frequent, but large cascading events involving many line outages are possible.

The dynamical behavior of this model has important implications for power system planning and operation and for the mitigation of blackout risk. The present model has some of the characteristic properties of an SOC system, although we cannot prove that is strictly the case. The success of mitigation efforts in SOC systems is strongly influenced by the dynamics of the system. One can understand SOC dynamics as including opposing forces that drive the system to a "dynamic equilibrium" near criticality in which disruptions of all sizes occur. Power tails are a characteristic feature of this dynamic equilibrium. Unless the mitigation efforts alter the self-organization forces driving the system, the system will be pushed to criticality. To alter those forces with mitigation efforts may be quite difficult because the forces are an intrinsic part of our society. Then the mitigation efforts can move the system to a new dynamic equilibrium while remaining near criticality and preserving the power tails.[5] Thus, while the absolute frequency of disruptions of all sizes may be reduced, the underlying forces can still cause the relative frequency of large blackouts to small blackouts to remain the same.

Acknowledgments

Ian Dobson and David Newman gratefully acknowledge support in part from NSF grants ECS-0216053 and ECS-0214369. Ian Dobson and B. A. Carreras gratefully acknowledge coordination of part of this work by the Consortium for Electric Reliability Technology Solutions and funding in part by the Assistant Secretary for Energy Efficiency and Renewable Energy, Office of Power Technologies, Transmission Reliability Program of the U.S. Department of Energy under contract 9908935 and Interagency Agreement DE-A1099EE35075 with the National Science Foundation. Part of this research has been carried out at Oak Ridge National Laboratory, managed by UT-Battelle, LLC, for the U.S. Department of Energy under contract number DE-AC05-00OR22725.

Appendix A

The blackout model is based on the standard DC power flow equation,

$$F = AP \quad , \tag{A-1}$$

where F is a vector whose N_L components are the power flows through the lines, F_{ij}, P is a vector whose N_N–1 components are the power of each node, P_i, with the exception of the reference generator, P_0, and A is a constant matrix. The reference generator power is not included in the vector P to avoid singularity of A as a consequence of the overall power balance.

The input power demands are either specified deterministically or as an average value plus some random fluctuation around the average value. The random fluctuation is applied to either each load or to "regional" groups of load nodes.

The generator power dispatch is solved using standard LP methods. Using the input power demand, we solve the power flow equations, Eq. (A-1), with the condition of minimizing the following cost function:

$$\text{Cost} = \sum_{i \in G} P_i(t) - W \sum_{j \in L} P_j(t) \quad . \tag{A-2}$$

We assume that all generators run at the same cost and that all loads have the same priority to be served. However, we set up a high price for load shed by setting W at 100. This minimization is done with the following constraints:

(1) Generator power $\quad 0 \le P_i \le P_i^{\max} \quad i \in G$

(2) Load power $\quad P_j \le 0 \quad j \in L$

(3) Power flows $\quad \left|F_{ij}\right| \le F_{ij}^{\max}$

(4) Power balance $\quad \sum_{i \in G \cup L} P_i = 0$

This linear programming problem is numerically solved by using the simplex method as implemented in.[25] The assumption of uniform cost and load priority can of course be relaxed, but changes to the underlying dynamics are not likely from this.

In solving the power dispatch problem for low-load power demands, the initial conditions are chosen in such a way that a feasible solution of the linear programming problem exists. That is, the initial conditions yield a solution without line overloads and without power shed. Increases in the average load powers and random load fluctuations can cause a solution of the linear programming with line overloads or requiring load power to be shed. At this point, a cascading event may be triggered.

A cascading overload may start if one or more lines are overloaded in the solution of the linear programming problem. We consider a line to be overloaded if the power flow through it is within 1% of $F_{ij}^{\max}$. At this point, we assume that there is a probability p_1 that an overloaded line will cause a line outage. If an overloaded line experiences an outage, we reduce its corresponding $F_{ij}^{\max}$ by a large amount (making it effectively zero) to simulate the outage, and calculate a new solution. This process can require multiple iterations and continues until a solution is found with no more outages.

This fast dynamics model does not attempt to capture the intricate details of particular blackouts, which may have a large variety of complicated interacting processes also involving, for example, protection systems, and dynamics and human factors. However, the fast dynamics model does represent cascading overloads and outages that are consistent with some basic network and operational constraints.

Table I

Number of nodes	PDF decay index	Range of power tail
46	-1.13	7
94	-1.16	17
190	-1.16	36
382	-1.21	62

References

[1]D. N. Ewart, IEEE Spectrum, **36** (1978).

[2]B. A. Carreras, D. E. Newman, I. Dobson, and A. B. Poole, "Evidence for self-organized criticality in electric power system blackouts," paper submitted to IEEE Transactions on Circuits and Systems Part I .

[3]J. Chen, J. S. Thorp, and M. Parashar, "Analysis of electric power disturbance data," 34th Hawaii International Conference on System Sciences, Maui, Hawaii, January 2001.

[4]Information on electric systems disturbances in North America can be downloaded from the NERC website at http://www.nerc.com/dawg/database.html.

[5]B. A. Carreras, V. Lynch, I. Dobson, and D. E. Newman, "Blackout mitigation assessment in power transmission systems," 36th Hawaii International Conference on System Sciences, Hawaii, January 2003.

[6]I. Dobson, B. A. Carreras, V. Lynch, and D. E. Newman, "An initial model for complex dynamics in electric power system blackouts," 34th Hawaii International Conference on System Sciences, Maui, Hawaii, January 2001.

[7]B. A. Carreras, D. E. Newman, I. Dobson, and A. B. Poole, "Modeling blackout dynamics in power transmission networks with simple structure," 34th Hawaii International Conference on System Sciences, Maui, Hawaii, January 2001.

[8]B. A. Carreras, V. Lynch, I. Dobson, and D. E. Newman, CHAOS, **12**, 985 (2002).

[9]P. Bak, C. Tang, and K. Wiesenfeld, Phys. Rev. Lett. **59**, 1987, pp. 381-4.

[10]M. L. Sachtjen, B. A. Carreras, and V. E. Lynch, Phys. Rev. E **61**, 4877 (2000).

[11]J. Chen and J. S. Thorp, "A reliability study of transmission system protection via a hidden failure DC load flow model," IEEE Fifth International Conference on Power System Management and Control, 17–19 April 2002, 384–389.

[12]J. Chen, J. S. Thorp, and I. Dobson, "Cascading dynamics and mitigation assessment in power system disturbances via a hidden failure model," preprint, submitted to International Journal of Electrical Power and Energy Systems, 2003.

[13]M. D. Stubna and J. Fowler, International Journal of Bifurcation and Chaos, **13** (1), 237 (2003).

[14] S. Roy, C. Asavathiratham, B. C. Lesieutre, and G. C. Verghese, "Network models: growth, dynamics, and failure," Proceedings of the 34th Annual Hawaii International Conference on System Sciences, January 3–6, 2001, pp. 728 –737.

[15]D. L. Pepyne, C. G. Panayiotou, C. G. Cassandras, and Y.-C. Ho, "Vulnerability assessment and allocation of protection resources in power systems," Proceedings of the American Control Conference, Vol. 6 , 25–27 June 2001, pp. 4705 –4710.

[16]C. L. DeMarco, "A phase transition model for cascading network failure," IEEE Control Systems Magazine, Vol. 21, No. 6, pp. 40–51, December 2001.

[17]P. A. Parrilo, S. Lall, F. Paganini, G. C. Verghese, B. C. Lesieutre, J. E. Marsden, "Model reduction for analysis of cascading failures in power systems," Proceedings of the 1999 American Control Conference, Vol. 6, 2–4 June 1999, pp. 4208–4212.

[18]B. Stott and E. Hobson, IEEE Trans. Power Appar. Syst., **PAS-97**, 1713 (1978).

[19]B. Stott and E. Hobson, IEEE Trans. Power Appar. Syst., **PAS-97**, 1721(1978).

[20]B. Stott and J. L. Marinho, IEEE Trans. Power Appar. Syst., **PAS-97**, 837 (1979).

[21]The IEEE 118 bus network model is a standard test system; see http://www.ee.washington.edu/research/pstca/.

[22]Statistical Yearbook of the electric utility industry/1998, published by Edison Electric Institute (1998).

[23]H. E. Hurst, Trans. Am. Soc. Civil Eng. **116**, 770 (1951).

[23]B. B. Mandelbrot and J. R. Wallis, Water Resources Research **4**, 909–918 (1969).

[25]W. H. Press, B. P. Flannery, S. A. Teukolsky, and W. T. Vetterling, *Numerical Recipes in C* (Cambridge University Press, Cambridge, 1988).

Figure captions

Fig. 1. Diagram of the IEEE 118 bus network. Generators are gray squares; loads are the black squares.

Fig. 2. Time evolution of the power served and number of blackouts per year from the model.

Fig. 3. R/S for the time series of normalized load shed and line outages for a 46-node tree network.

Fig. 4. The Hurst exponent H as a function of Γ for the time series of normalized load shed (a) and line outages (b). The exponent is calculated from a fit of R/S in the time range $600 \leq t \leq 10^5$ for 46, 94, and 190 nodes tree networks and for the IEEE 118 bus network.

Fig. 5. PDF of the load shed normalized to the total power demand for three different tree networks. The PDFs obtained from a load scan near the critical point are compared with the PDF obtained from the dynamical model discussed in this paper.

Fig. 6. PDF of the normalized load shed for the 382-node tree, the IEEE 118 bus networks, and the North American blackouts in 15 years of NERC data normalized to the largest blackout.

Fig. 7: Averaged power delivered and number of line outages per blackout for the 94-node tree network as a function of Γ.

Fig. 8: PDF of the number of outages per blackout for the 94-node tree network for different values of Γ.

Fig. 9: Ratio of the frequency of blackouts with more than 15 outages to the frequency of blackouts for the 94-node tree network as a function of Γ.

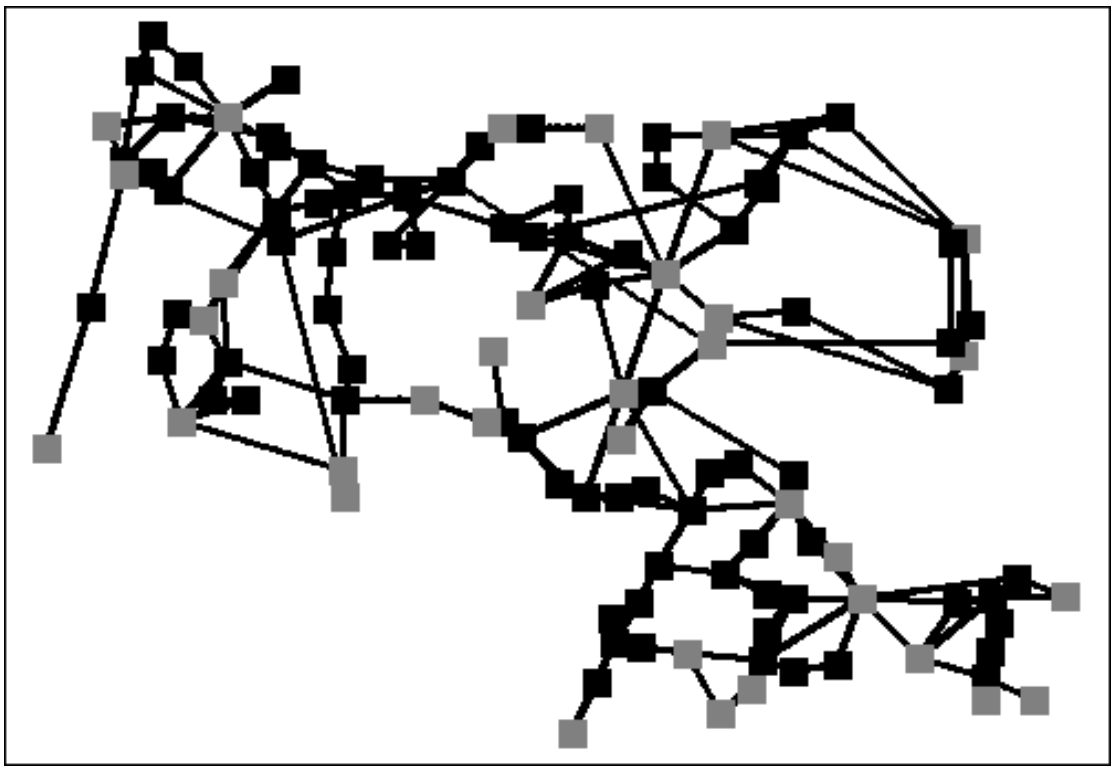

Fig. 1

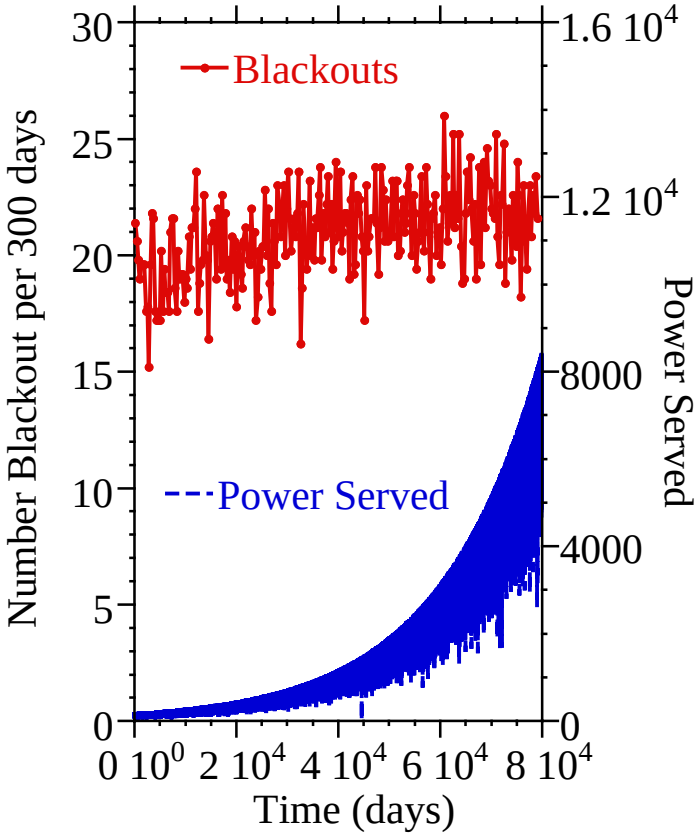
Blackouts
Power Served
Number Blackout per 300 days
Power Served
Time (days)
0
5
10
15
20
25
30
0
4000
8000
1.2 10^4
1.6 10^4
0 10^0 2 10^4 4 10^4 6 10^4 8 10^4

Fig. 2

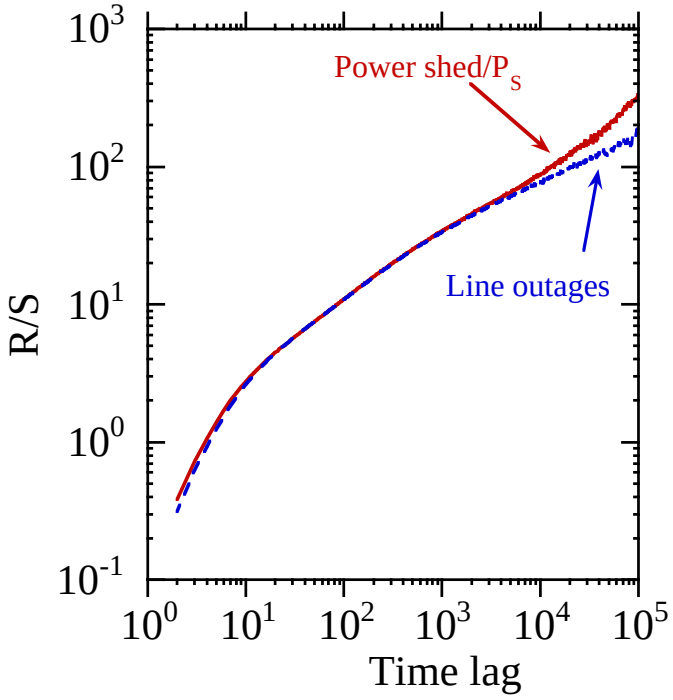
Power shed/P_S
Line outages
R/S
Time lag
10^3
10^2
10^1
10^0
10^-1
10^0
10^1
10^2
10^3
10^4
10^5

Fig. 3

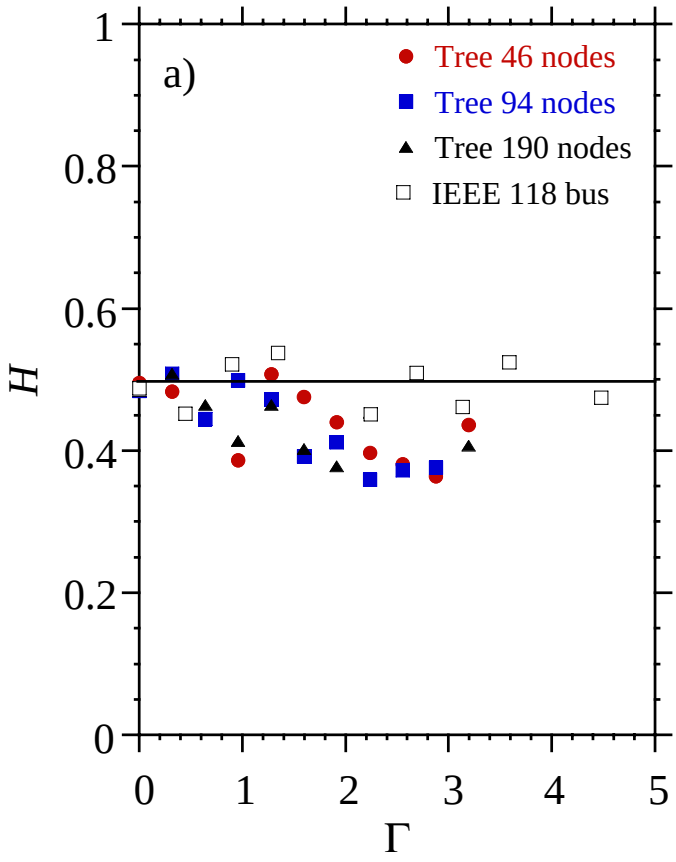
a)
Tree 46 nodes
Tree 94 nodes
Tree 190 nodes
IEEE 118 bus
H
Γ
0
0.2
0.4
0.6
0.8
1
0
1
2
3
4
5

Fig, 4a

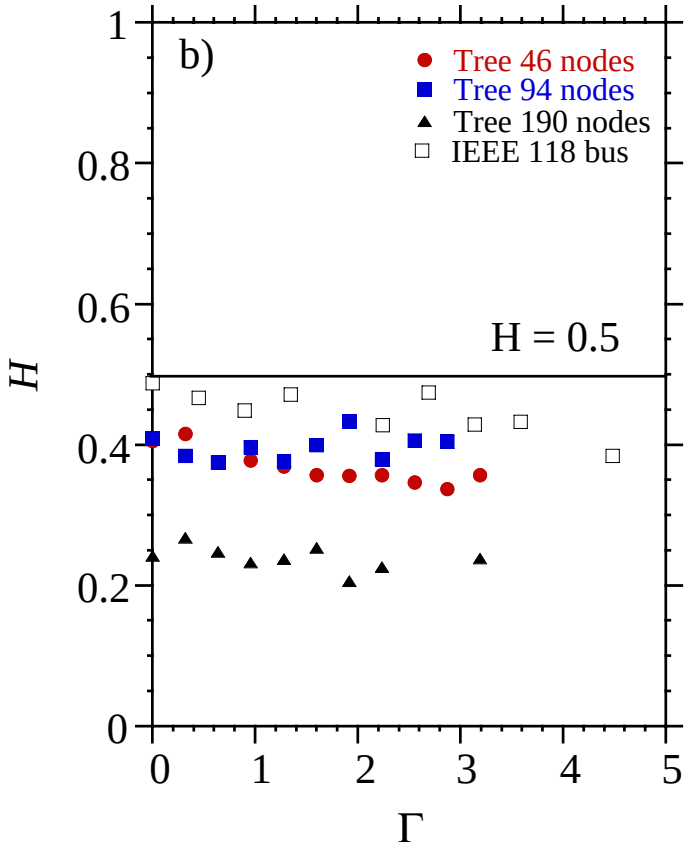
b)
Tree 46 nodes
Tree 94 nodes
Tree 190 nodes
IEEE 118 bus
H = 0.5
H
Γ
0
0.2
0.4
0.6
0.8
1
0
1
2
3
4
5

Fig. 4b

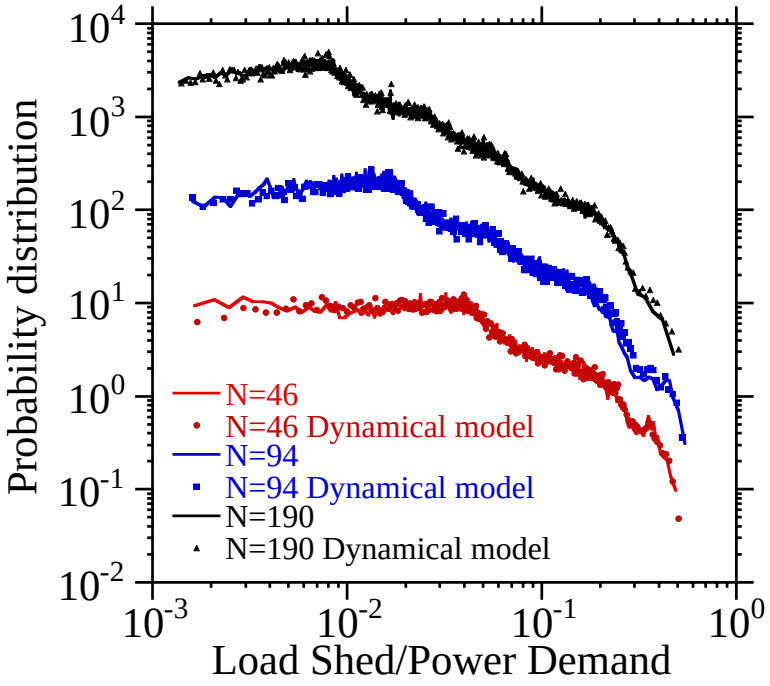
Probability distribution
Load Shed/Power Demand
N=46
N=46 Dynamical model
N=94
N=94 Dynamical model
N=190
N=190 Dynamical model

Fig. 5

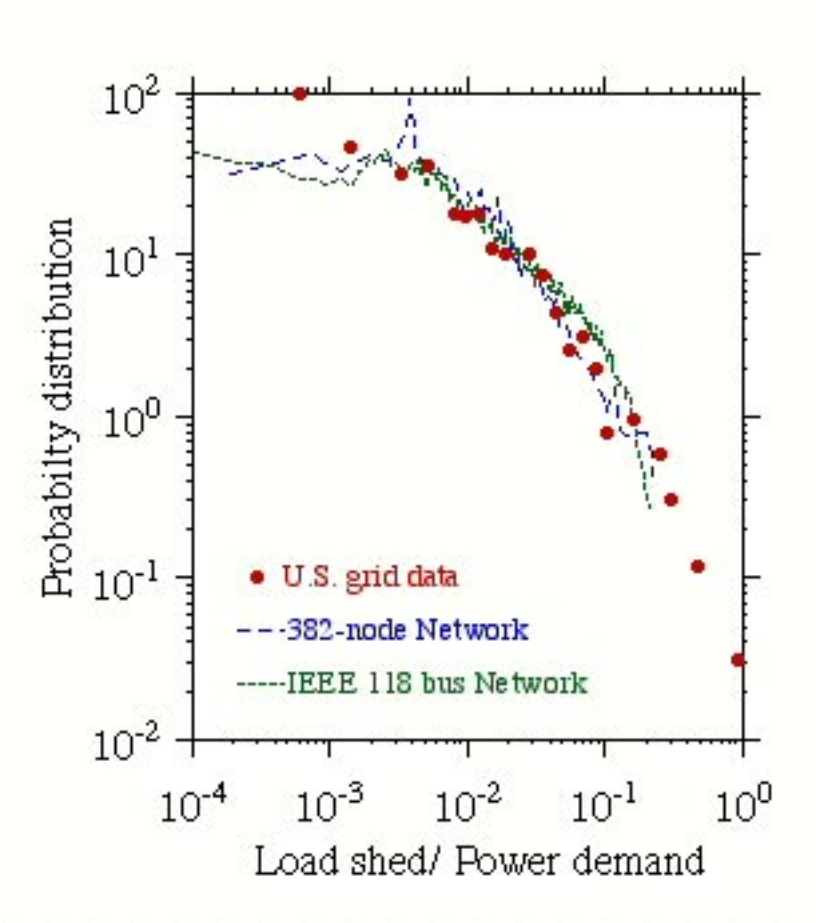
Probabilty distribution
Load shed/ Power demand
U.S. grid data
382-node Network
IEEE 118 bus Network

Fig. 6

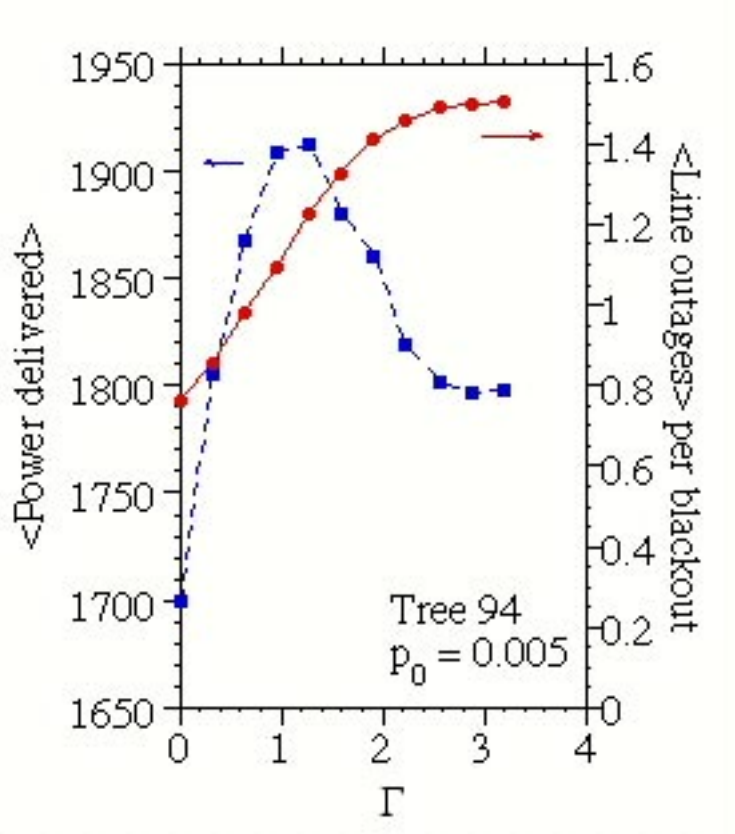
<Power delivered>
<Line outages> per blackout
Γ
Tree 94
$p_0 = 0.005$
1950
1900
1850
1800
1750
1700
1650
1.6
1.4
1.2
1
0.8
0.6
0.4
0.2
0
0
1
2
3
4

Fig. 7

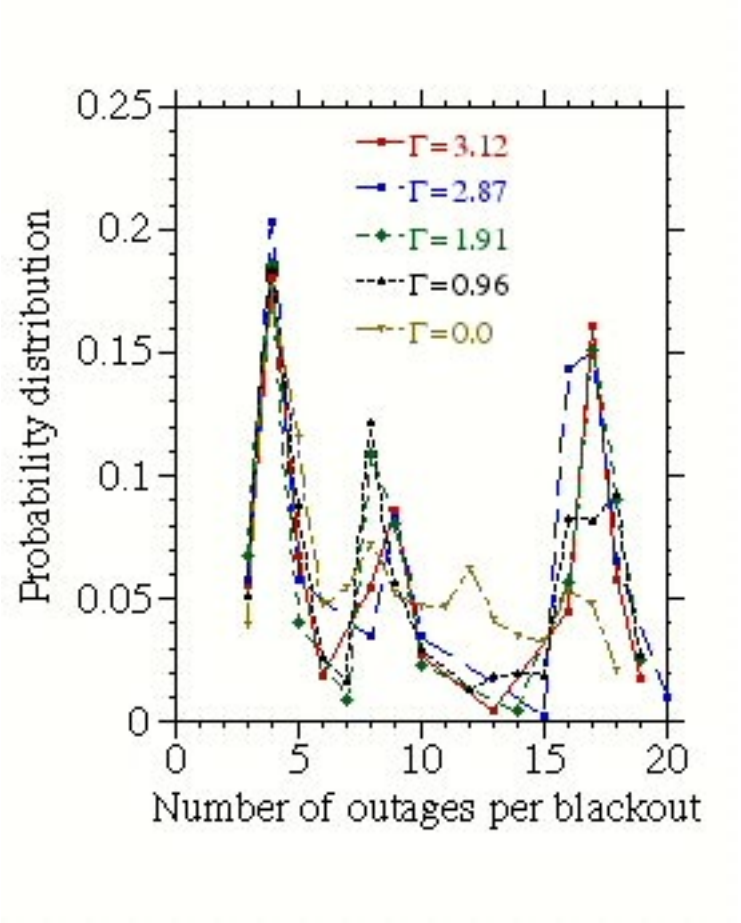
0.25
0.2
0.15
0.1
0.05
0
Probability distribution
Γ=3.12
Γ=2.87
Γ=1.91
Γ=0.96
Γ=0.0
0
5
10
15
20
Number of outages per blackout

Fig. 8

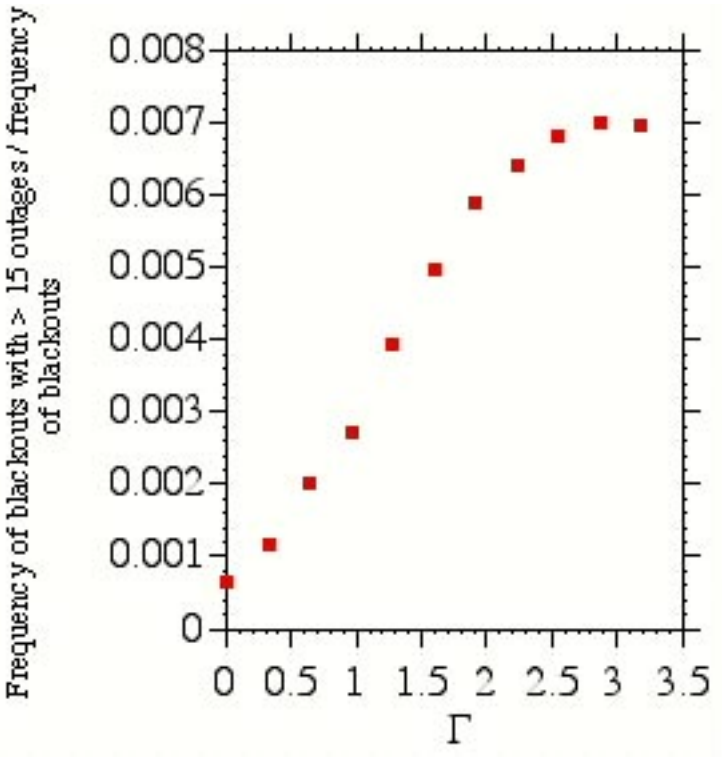
Frequency of blackouts with > 15 outages / frequency of blackouts
0.008
0.007
0.006
0.005
0.004
0.003
0.002
0.001
0
0 0.5 1 1.5 2 2.5 3 3.5
Γ

Fig 9